

Geophysical Research Letters®

RESEARCH LETTER

10.1029/2023GL103428

Key Points:

- Summer precipitation isotopes in the Arctic reflect temperature and moisture transport history
- Paired records of summer temperature and precipitation isotopes isolate the influence of temperature from that of transport
- Moisture delivery to the eastern Canadian Arctic changed dramatically due to Early Holocene Laurentide Ice Sheet retreat

Supporting Information:

Supporting Information may be found in the online version of this article.

Correspondence to:

E. K. Thomas,
ekthomas@buffalo.edu

Citation:

Thomas, E. K., Cluett, A. A., Erb, M. P., McKay, N. P., Briner, J. P., Castañeda, I. S., et al. (2023). Early Holocene Laurentide Ice Sheet retreat influenced summer atmospheric circulation in Baffin Bay. *Geophysical Research Letters*, 50, e2023GL103428. <https://doi.org/10.1029/2023GL103428>

Received 7 MAR 2023

Accepted 1 JUN 2023

Early Holocene Laurentide Ice Sheet Retreat Influenced Summer Atmospheric Circulation in Baffin Bay

Elizabeth K. Thomas¹ , Allison A. Cluett^{1,2,3,4} , Michael P. Erb² , Nicholas P. McKay² , Jason P. Briner¹ , Isla S. Castañeda⁵, Megan C. Corcoran^{1,6} , Owen C. Cowling¹ , Devon B. Gorbey¹ , Kurt R. Lindberg¹ , Karlee K. Prince¹, and Jeffrey Salacup⁵ 

¹University at Buffalo, Buffalo, NY, USA, ²Northern Arizona University, Flagstaff, AZ, USA, ³Now at University of California, Santa Cruz, Santa Cruz, CA, USA, ⁴Now at NOAA Southwest Fisheries Science Center, La Jolla, CA, USA,

⁵University of Massachusetts Amherst, Amherst, MA, USA, ⁶Now at University of Cincinnati, Cincinnati, OH, USA

Abstract Changes in ice-sheet size impact atmospheric circulation, a phenomenon documented by models but constrained by few paleoclimate records. We present sub-centennial-scale records of summer temperature and summer precipitation hydrogen isotope ratios ($\delta^2\text{H}$) spanning 12–7 ka from a lake on Baffin Island. In a transient model simulation, winds in this region were controlled by the relative strength of the high-pressure systems and associated anticyclonic circulation over the retreating Greenland and Laurentide ice sheets. The correlation between summer temperature and precipitation $\delta^2\text{H}$ proxy records changed from negative to positive at 9.8 ka. This correlation structure indicates a shift from alternating local and remote moisture, governed by the two ice-sheet high-pressure systems, to only remote moisture after 9.8 ka, governed by the strong Greenland high-pressure system after the Laurentide Ice Sheet retreated. Such rapid atmospheric circulation changes may also occur in response to future, gradual ice-sheet retreat.

Plain Language Summary Continental ice sheets alter atmospheric circulation, influencing global heat and moisture distribution. Records of atmospheric circulation during previous periods of ice-sheet retreat can provide insights into the changes that are possible in the future. This study examines summer atmospheric circulation in Baffin Bay from 12,000 to 7,000 years ago, a period of dramatic ice-sheet retreat. Precipitation isotopes reflect moisture source, which responds to changes in air temperature and atmospheric circulation. This study uses records of temperature and precipitation isotopes from the same sediment archive to tease apart the influence of temperature from that of atmospheric circulation. The precipitation isotopes in this record distinct changes in moisture sources, which a climate model simulation suggests was caused by retreating ice sheets. Before about 10 ka, when the Laurentide Ice Sheet (LIS) covered eastern Canada, summer winds in Baffin Bay shifted regularly between south and north, carrying air with unique temperature and precipitation isotope signatures. As the LIS retreated, the Greenland Ice Sheet (GIS) remained relatively large and dominated atmospheric circulation, causing a rapid shift to southeasterly winds. As the GIS retreats in the future, atmospheric circulation may undergo similar rapid changes.

1. Introduction

As Earth warms, the amount and residence time of atmospheric moisture increase, enhancing long-distance moisture transport, and causing wetter Arctic summers (Arctic Report Card, 2022; Singh et al., 2017). A wetter Arctic impacts ocean circulation, permafrost, plant communities, and carbon storage (Bring et al., 2016; Serreze et al., 2006; Vihma et al., 2016). Today, high-elevation cold air causes high atmospheric pressure over the Greenland Ice Sheet (GIS), promoting anticyclonic circulation around the GIS and poleward moisture transport via storm tracks over the Labrador Sea (Dufour et al., 2016). Yet, the importance of regional dynamics in the context of hemispheric changes in temperature gradients and moisture residence time is not well constrained. Although the GIS influence on atmospheric circulation is not likely to change on short (annual to decadal) time scales, ice-sheet-caused change may be important on longer (centennial to millennial) time scales.

Past continental ice sheets influenced atmospheric circulation. The size and position of the Laurentide Ice Sheet (LIS) influenced the configuration of the jet stream (Löfverström et al., 2014), bringing warmth to Beringia during the Last Glacial Maximum (LGM) (Tulenko et al., 2020), changing the location of moisture delivery to Eurasia (Kageyama & Valdes, 2000; Liakka et al., 2016) and increasing long-distance atmospheric transport to

© 2023 The Authors.

This is an open access article under the terms of the Creative Commons Attribution-NonCommercial License, which permits use, distribution and reproduction in any medium, provided the original work is properly cited and is not used for commercial purposes.

the Canadian Arctic (McAndrews, 1984). A roughly 150-km-wide band of anticyclonic winds around the LIS shifted during deglaciation, causing changes in prevailing wind direction that impacted sand spit formation and lake effect snowfall in the Laurentian Great Lakes (Griggs et al., 2022; Schaetzl et al., 2016). During the Early Holocene, when the LIS was significantly reduced from its LGM size but still retreating, this anticyclonic circulation continued to influence areas around its margins (Gregoire et al., 2018). More paleoclimate records in regions affected by ice-sheet change and spanning the Early Holocene may reveal the nature and rate of atmospheric response to ice-sheet change.

Precipitation stable isotopes ($\delta^{18}\text{O}$, $\delta^2\text{H}$) reflect changes in the water cycle. Three primary factors influence precipitation isotope values at low-elevation coastal Arctic sites: (a) The temperature at the site of precipitation, (b) The temperature at the source location(s), and (c) The isotopic composition of the vapor at the source location(s) (I. D. Clark & Fritz, 1997; Gaglioti et al., 2017). Because an air parcel's moisture evaporates and condenses during transport, the isotope value of precipitation is a function of conditions throughout the transport history, and generally becomes more ^2H - and ^{18}O -depleted with longer transport times (Gimeno et al., 2021; Steen-Larsen et al., 2015).

When moisture sources are constant, local temperature is typically the dominant mechanism controlling precipitation isotope values (Figure S1 in Supporting Information S1) (Berrisford et al., 2011; Cluett et al., 2021; Putman et al., 2017; Vinnikov et al., 2011). In contrast, varying moisture sources through time can cause large changes in precipitation isotope values that overprint the local temperature signal. This occurs both on intra-annual time scales (Cluett et al., 2021; Putman et al., 2017; Sodemann et al., 2008; Steen-Larsen et al., 2015) and on decadal to orbital time scales (He et al., 2021; LeGrande & Schmidt, 2009; Masson-Delmotte et al., 2005; Thomas et al., 2014; White et al., 1997). Paired but independent proxy records of temperature and precipitation isotopes can isolate the influence of local temperature, providing insight into changing moisture sources and atmospheric circulation (Thomas et al., 2014, 2018).

The Clyde Foreland, our study area, is a low-lying coastal area on northeastern Baffin Island, eastern Canadian Arctic. LIS retreat from this foreland around 14 ka (Briner et al., 2005; Young et al., 2012), revealed lakes that provide rare archives spanning the entire Holocene (Axford et al., 2009; Briner et al., 2007). Peak summer temperature up to 5°C warmer than the pre-Industrial occurred in the Early Holocene in the Baffin Bay region, nearly in phase with peak Northern Hemisphere summer insolation (Axford et al., 2009, 2021; Environment and Climate Change Canada, 2011; Kobashi et al., 2017; Lecavalier et al., 2017; Pendleton et al., 2019). This warmth occurred despite the much larger LIS, which lost 50% of its area (compared to its extent at 21 ka) between 13 and 6 ka (Briner et al., 2009; Dalton et al., 2020). Today, a low-pressure system in the eastern Canadian Arctic causes cyclonic circulation in summer (Figure 1g) (Hersbach et al., 2020), carrying moisture from high-latitude continental North America to Baffin Island.

We generate sub-centennial-resolution late-glacial to Early Holocene records of summer temperature and summer precipitation $\delta^2\text{H}$ values on the Clyde Foreland using two separate classes of lipid biomarkers. For this study, “summer” means the lake-ice-free season when these lipid biomarkers are produced in the lake, which today is July, August, and September. We assess the stability of moisture sources through this period by examining the correlation structure between summer temperature and precipitation $\delta^2\text{H}$. These results, in conjunction with a transient general circulation model simulation (Liu et al., 2009), allow us to test the hypothesis that Early Holocene atmospheric circulation in the Baffin Bay region was influenced by LIS retreat.

2. Methods

We present organic geochemical records from a radiocarbon-dated sediment core from Lake CF8 on the Clyde Foreland (Figure 2; Figures S2 and S3, Table S1, and Text S1.2 in Supporting Information S1) (Axford et al., 2009; Blaauw & Christen, 2011; Crump et al., 2021; Reimer et al., 2020; Wilson et al., 2012). Ten aquatic moss macrofossils, which in this region are in equilibrium with the atmosphere (Snyder et al., 2013; Wolfe et al., 2004), and two stratigraphic constraints form the basis for the age-depth model (Text S1.2 in Supporting Information S1). We extracted, purified, and analyzed free lipids from freeze-dried sediments (Hopmans et al., 2016; Thomas et al., 2018, 2020) (Text S1.3 and Table S2 in Supporting Information S1). We used GeoChronR for statistical analyses (Text S1.4 in Supporting Information S1) (Kaiser, 1958; McKay et al., 2021; Richman, 1986).

We use branched glycerol dialkyl glycerol tetraethers (brGDGTs), which we interpret as lacustrine, to infer summer temperature, using a calibration to *in situ* lake water temperature on southern Greenland with a similar seasonal

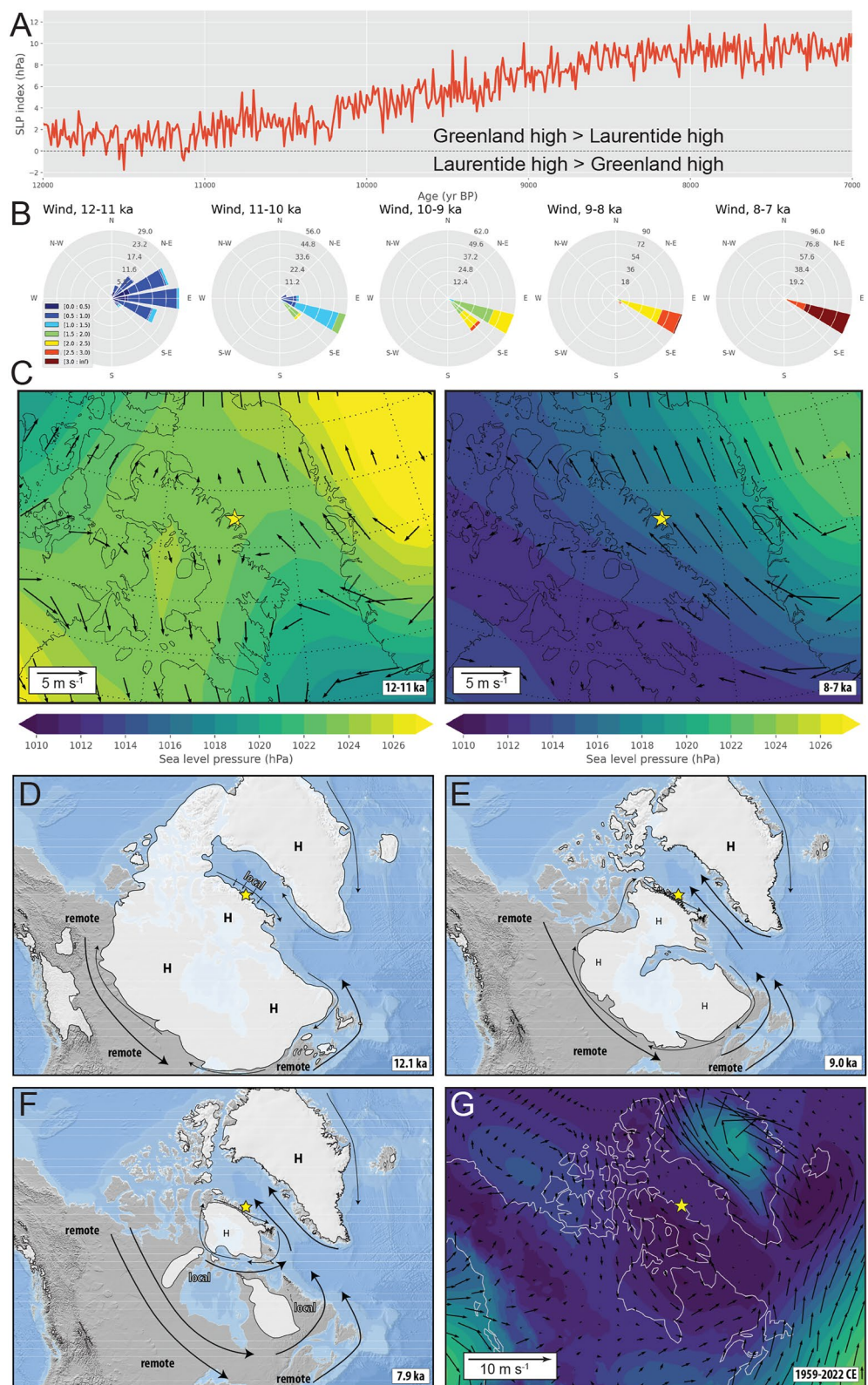


Figure 1.

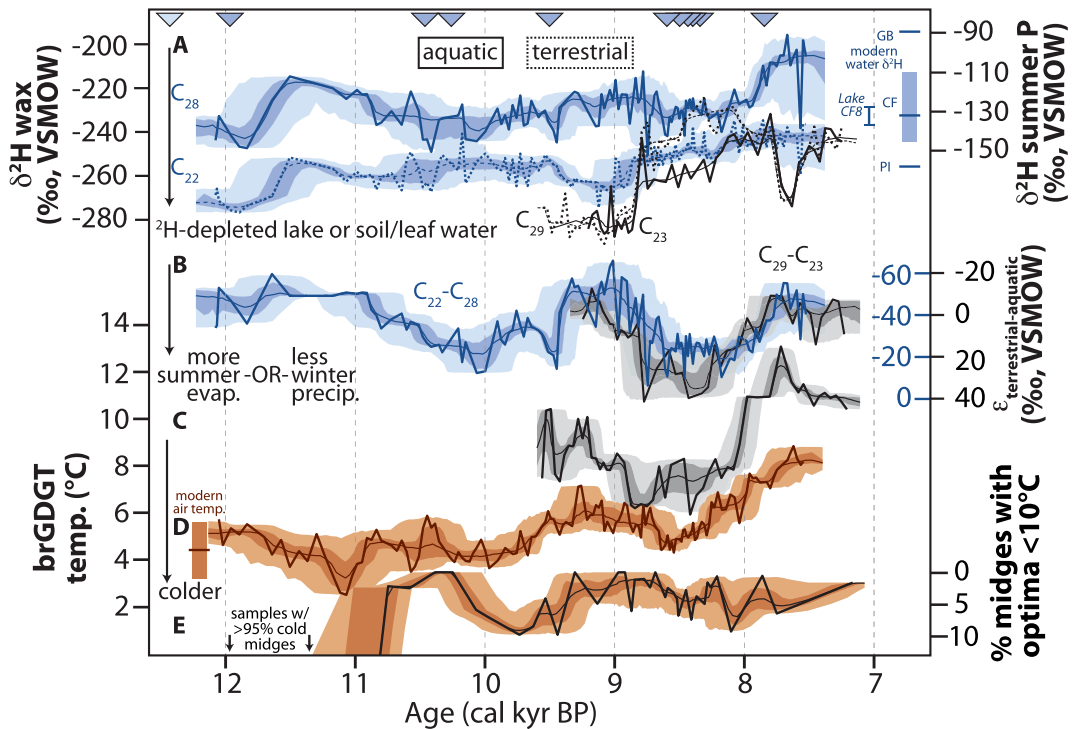


Figure 2. Early Holocene records from lakes CF8, Baffin Island (blue/orange) and Sikuiui, western Greenland (black) (Thomas et al., 2018). (a) Leaf wax $\delta^2\text{H}$ values (Texts S3.1 and S3.2 in Supporting Information S1), dashed: terrestrial (CF8: C_{22} *n*-alkanoic acid, Sikuiui: C_{29} *n*-alkane), solid: aquatic (CF8: C_{28} *n*-alkanoic acid, Sikuiui: C_{23} *n*-alkane); Right axis: Leaf wax $\delta^2\text{H}$ values converted to precipitation $\delta^2\text{H}$ (Text S1.6 in Supporting Information S1); observed (GB, Goose Bay; PI, Pond Inlet) and modeled (CF, Clyde Foreland) summer precipitation $\delta^2\text{H}$, mean $\delta^2\text{H}$ of Lake CF8 water. (b) Difference between terrestrial and aquatic leaf wax $\delta^2\text{H}$ ($\epsilon_{\text{terrestrial-aquatic}}$); (c) Sikuiui Lake brGDGT-inferred summer temperature; (d) Lake CF8 brGDGT-inferred summer temperature; (e) Percent cold stenotherm chironomid midges at Lake CF8 (reversed y-axis), two samples with values $>95\%$ are shown with arrows. Triangles: age control points (Table S1 in Supporting Information S1). For all records, light and dark shading: 95th percentile and interquartile age uncertainty, respectively, fine line: median age uncertainty, bold line: record on median modeled age.

climate as Lake CF8 (Zhao et al., 2021). We discuss brGDGT sources and the choice of temperature calibration in Texts S2.2 and S3.1 (Table S3 and Figures S4–S7) in Supporting Information S1 (Blaga et al., 2009; Cluett et al., 2023; Daniels et al., 2022; De Jonge, Hopmans, et al., 2014; De Jonge, Stadnitskaia, et al., 2014; Hopmans et al., 2004; Huguet et al., 2006; Martínez-Sosa & Tierney, 2019; Martínez-Sosa et al., 2021; Naafs et al., 2017; Raberg et al., 2021; Rohling & Pälike, 2005; Russell et al., 2018; Schouten et al., 2013; Yao et al., 2020).

We interpret the C_{28} *n*-alkanoic acid in Lake CF8 as predominantly aquatic and the C_{22} *n*-alkanoic acid as at least partially terrestrial, based on similar chain-length distributions with submerged aquatic mosses, the most abundant plant in the catchment, and different trends in $\delta^2\text{H}$ values for different chain lengths (Text S3.3 and Figure S8 in Supporting Information S1). Lake CF8 water $\delta^2\text{H}$ values match summer precipitation, with no evaporative enrichment (Text S3.2 and Figure S2 in Supporting Information S1) (Bowen, 2016; Bowen et al., 2005; Chiasson-Poirier et al., 2020; Gibson & Edwards, 2002; Gorbey et al., 2022; IAEA/WMO, 2011; Jonsson et al., 2009; Zhao et al., 2022). Hereafter, we primarily discuss $\delta^2\text{H}_{C28}$, which we convert to summer precipitation $\delta^2\text{H}$ using an apparent fractionation factor derived from aquatic plants in Qaupat Lake, southern Baffin Island (Text S1.6 in Supporting Information S1) (Gorbey et al., 2022; Guo et al., 2013; Hollister et al., 2022; McFarlin et al., 2019).

Figure 1. Early Holocene ice sheet configuration and winds. (a–c) TraCE-21k results (Liu et al., 2009). (a) Decadal-mean JJA sea-level-pressure index between Laurentide and Greenland ice sheets (Figure S9 in Supporting Information S1). (b) Wind strength and direction over the Clyde Foreland during 1-Kyr-intervals. (c) Sea level pressure (shading) and winds (arrows) during 12–11 and 8–7 ka. (d–f) North American Ice sheet position through the Early Holocene (Dalton et al., 2020) and schematic of high-pressure location, wind direction, and moisture source locations to northeastern Baffin Island. (g) ERA5 (1959–2022) JJA sea level pressure and winds, shading as in panel (c) (Hersbach et al., 2020). Stars: Lake CF8. H: High pressure.

We used publicly available data from the 21,000-year-long transient simulation of the Community Earth System Model, TraCE-21k (Liu et al., 2009). We examined wind vectors and moisture flux at the four grid cells nearest Lake CF8. We quantified the difference in sea level pressure between the grid cells at the highest point on the GIS and LIS at 12 ka (Figure S9 in Supporting Information S1), to provide a metric for the pressure differential between the retreating LIS and the relatively stable GIS.

3. Results

Branched GDGTs and *n*-alkanoic acids C₂₀ through C₃₂ with high carbon preference index (4.3 ± 0.8) occurred in all samples that we analyzed (Figures S4 and S8 in Supporting Information S1) (Blaga et al., 2009; Cluett et al., 2023; Daniels et al., 2022; Marzi et al., 1993; Schouten et al., 2013). $\delta^2\text{H}_{\text{C}28}$ -inferred summer precipitation $\delta^2\text{H}$ and brGDGT-inferred summer temperature exhibit centennial- and millennial-scale variability consistent with regional records (Figure 2; Texts S2 and S3 in Supporting Information S1).

To better understand the mechanisms influencing summer precipitation $\delta^2\text{H}$, we compare Lake CF8 $\delta^2\text{H}_{\text{C}28}$ values and brGDGT-inferred temperatures, which are measured in the same samples, therefore their relationship is independent of age model uncertainty. Both proxies are produced in the lake throughout the ice-free season, and therefore reflect the same seasonality, even if the ice-free season length changes (Text S3 in Supporting Information S1). Summer precipitation $\delta^2\text{H}$ and temperature are negatively correlated on both millennial and centennial time scales prior to 9.8 ka, and positively correlated only on millennial time scales after 9.8 ka (Figure 3; Figure S10 and Table S4 in Supporting Information S1).

To explore the role of changing summer moisture sources at Lake CF8, we examine simulated decadal-mean summer conditions in TraCE-21k. The difference in modeled sea level pressure between the GIS and LIS was low from 12 to 11 ka, but increased thereafter (Figure 1a). Simulated summer wind speed and direction on northeastern Baffin Island changed at 11 ka (Figure 1b). Before 11 ka, surface winds were weak (<1 m/s), and were easterly or northeasterly. After 11 ka, surface winds gradually strengthened and became consistently southeasterly. Similarly, decadal-mean total-column summer moisture flux (which does not quantify sub-decadal eddies) strengthened and became more persistently southeasterly after 11 ka (Figure S11 in Supporting Information S1).

4. Discussion

4.1. Interpretive Framework

4.1.1. Biomarker Interpretations

We interpret Lake CF8 brGDGT-inferred temperature to reflect regional summer air temperature, as is common in Arctic lakes (Text S3.1 in Supporting Information S1) (Allegrucci et al., 2012; Buzert et al., 2018; Chen et al., 2022; Delettre, 1988; Denton et al., 2005; de Wet et al., 2016; Francis et al., 2006; Green & Sánchez, 2006; Halamka et al., 2023; Keisling et al., 2017; Kusch et al., 2019; Lindberg et al., 2022; Livingstone & Lotter, 1998; MacIntyre et al., 2009; Raberg et al., 2021; Shanahan et al., 2013; Thomas et al., 2018; Wu et al., 2021; Zhang et al., 2016; Zhao et al., 2021). We interpret $\delta^2\text{H}$ of the C₂₈ *n*-alkanoic acid from Lake CF8 to reflect summer lake water $\delta^2\text{H}$ values, which in turn reflect summer precipitation $\delta^2\text{H}$ values (Texts S3.2 and S3.3 in Supporting Information S1) (Faber et al., 2017; Gao et al., 2011; Gorbey et al., 2022; Johnsen et al., 2001; Paterson et al., 1977; Rach et al., 2014; Sachse et al., 2012; Thomas et al., 2020; van Bree et al., 2018). The difference between $\delta^2\text{H}$ of terrestrial and aquatic waxes, $\epsilon_{\text{terrestrial-aquatic}}$, reflects changes in the amount of snow melt contributing to soil water and/or changes in evaporation from soil or leaf water (Text S3.3.2 in Supporting Information S1).

4.1.2. Dynamical Controls and Isotope Characteristics of Moisture Sources to the Clyde Foreland

We interpret precipitation isotope values to reflect temperature and moisture transport history, and expect temperature and precipitation isotope values to be positively correlated when moisture sources are constant. When moisture sources vary, this relationship should weaken. Following this framework, the negative correlation between summer temperature and precipitation $\delta^2\text{H}$ at Lake CF8 before 9.8 ka suggests that summer moisture sources to the Clyde Foreland changed throughout this period. In contrast, the strong positive correlation between these same records after 9.8 ka suggests that local temperature is the dominant factor influencing summer precipitation $\delta^2\text{H}$, and moisture sources were constant at this time. Next, we describe likely moisture sources to the Clyde Foreland and the mechanisms that could cause changes in moisture source contributions through time.

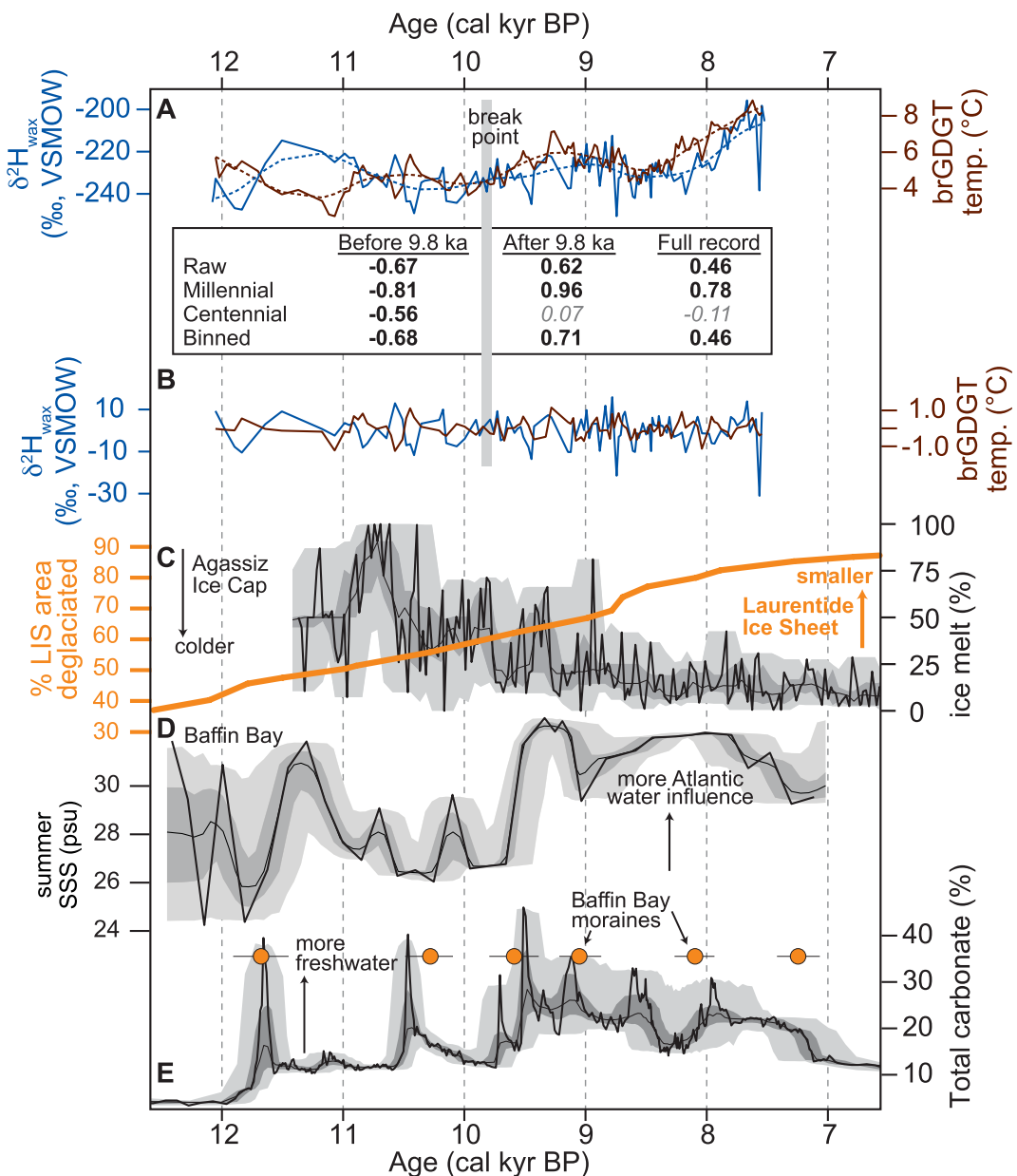


Figure 3. Early Holocene atmospheric and oceanic conditions in Baffin Bay. (a) Lake CF8 $\delta^2\text{H}_{\text{C}28}$ (blue) and brGDGT-inferred temperature (brown) for the raw record (solid) and for millennial-scale smooth splines (dashed). (b) Filtered centennial-scale record, as in (a). Gray rectangle shows the break point, before which correlation is negative, after which correlation is positive or weak. (c) Agassiz Ice Cap percent melt (black), a proxy for peak summer warmth (Lecavalier et al., 2017) and Laurentide Ice Sheet size relative to its extent at 21 ka (orange) (Dalton et al., 2020). (d) Baffin Bay Summer sea surface salinity (Gibb et al., 2015). (e) Total carbonate deposited on Cartwright Saddle (Jennings et al., 2015) and age of moraine sets deposited by mountain glaciers and ice sheets in Baffin Bay (orange dots) (Young et al., 2020). Inset. Correlation statistics for Lake CF8 $\delta^2\text{H}_{\text{C}28}$ and brGDGT-inferred temperature, bold black text = p -value < 0.001 . (c-e) Light and dark shading: 95th percentile and interquartile age uncertainty, respectively, fine line: median age uncertainty, bold line: record on median of age models.

During the late glacial and earliest Holocene, the LIS was retreating but still covered most of eastern Canada (Figures 1d and 3c). At this time, the high-pressure systems over both the LIS and GIS, and resulting anticyclonic circulation, were important for regional-scale circulation and moisture transport into Baffin Bay (Figures 1a–1c; Figure S11 in Supporting Information S1). Areas within 150 km of the LIS edge would have been impacted by the LIS anticyclonic circulation (Griggs et al., 2022; Kopec et al., 2014; Schaetzl et al., 2016), causing northwesterly

winds on the Clyde Foreland. The high-pressure system over the GIS was also strong during the Early Holocene, and would have caused southeasterly winds that carried remote moisture from North America to the Baffin Bay region (Cluett et al., 2021; Nusbaumer et al., 2020).

The relative strength of these two high-pressure systems through time controlled the position of the boundary between the northwesterly and southeasterly winds, which influenced the source of moisture to northeastern Baffin Island (Figures 1a–1c; Figure S11 in Supporting Information S1). A stronger high over the LIS caused northwesterly winds to carry Arctic air masses to Baffin Island. Cold and dry Arctic air masses would carry minimal moisture to the Clyde Foreland. In contrast, a stronger high over the GIS caused southeasterly winds carrying warm, moist air masses from lower latitudes to this region. The long-distance moisture transport from low latitudes would yield relatively $\delta^2\text{H}$ -depleted precipitation coincident with warm air masses. Due to the persistence of the GIS and the disappearance of the LIS during the Holocene, we expect a relative strengthening of the GIS high-pressure system, and a concomitant increase in southeasterly winds, throughout this time (Figures 1d–1f).

In addition to regional-scale circulation, sea breezes that occur on small spatial and temporal scales may have been an important source of moisture to Baffin Island during the Early Holocene, as they are to western Greenland today (Kopec et al., 2014). When the LIS was large, the Clyde Foreland likely experienced strong daily transitions between katabatic winds coming off the LIS and sea breezes from Baffin Bay. Strong sea breezes occur when the land is warmer than the sea, causing a local low pressure over land. Modern on-shore breezes on Greenland are humid and $\delta^2\text{H}$ -enriched relative to katabatic winds (Kopec et al., 2014). Thus, when cold, dry Arctic air masses dominated the large-scale atmospheric circulation on eastern Baffin Island, sea breezes would have been the primary source of moisture to the Clyde Foreland. Because sea breezes carry moisture from local lake and land sources (Kopec et al., 2014), this moisture is minimally distilled, and therefore $\delta^2\text{H}$ -enriched, relative to moisture from remote sources. Mid- and high-latitude water bodies are not important sources of moisture to this region in summer (Cluett et al., 2021; Nusbaumer et al., 2020), so $\delta^2\text{H}$ -depletion of these water bodies caused by freshwater from melting ice sheets likely minimally impacted summer precipitation $\delta^2\text{H}$ values. Next, we use this mechanistic framework to interpret the Lake CF8 $\delta^2\text{H}$ record.

4.2. Mechanisms Controlling Early Holocene Summer Precipitation $\delta^2\text{H}$ on Northeastern Baffin Island

4.2.1. The Younger Dryas and Earliest Holocene

From 12.1 to 9.8 ka, the Lake CF8 record is characterized by anticorrelation between summer temperature and precipitation $\delta^2\text{H}$: when temperature increases, precipitation becomes $\delta^2\text{H}$ -depleted (Figures 3a and 3b). We interpret this anticorrelation to indicate frequent shifts between the dominance of remote and local moisture (Figure 1d). When the GIS high-pressure system dominated, southeasterly winds carried warm, moist air masses, which contained strongly distilled, $\delta^2\text{H}$ -depleted vapor to Baffin Island. When the LIS high-pressure system dominated, northwesterly winds carried cold, dry air masses to the region, increasing the relative importance of local moisture delivered by sea breezes and resulting in $\delta^2\text{H}$ -enriched precipitation. This interpretation is supported by the TraCE-21k simulation, which shows that the high pressure over the two ice sheets is roughly equal before 11 ka, and the Clyde Foreland is close to the boundary between the winds circulating around the two high-pressure systems (Figures 1a and 1c). During this time, summer winds on the Clyde Foreland were weak and their direction varied dramatically from one decade to the next, reflecting the time-varying dominance of the two ice-sheet high-pressure systems. The position of the boundary between ice-sheet high-pressure systems and the dominance of a given ice sheet was probably governed by stochastic interdecadal variability. The $\varepsilon_{\text{terrestrial-aquatic}}$ suggests either low, then increasing summer evaporation prior to 9.8 ka or decreasing influence of winter precipitation (Figure 2b).

Two of the intervals with relatively cool and $\delta^2\text{H}$ -enriched summer precipitation at Lake CF8 (11.7 and 10.5 ka) coincided with carbonate deposition events in the Labrador Sea (Figures 3a, 3b, and 3e) (Jennings et al., 2015). These freshwater events caused regional cold conditions (Young et al., 2020), which in turn may have caused enhanced northwesterly winds and local moisture dominance.

4.2.2. From 9.8 to 7.5 ka

The remainder of the Lake CF8 record is characterized by positive correlation between summer temperature and precipitation $\delta^2\text{H}$ on millennial time scales, but a lack of correlation on centennial time scales (Figures 3a

and 3b). The positive correlation at millennial timescales indicates the moisture sources to the Clyde Foreland were stable through this interval. Early Holocene air temperature was relatively stable in the moisture source regions (Figure 1e; Figure S12 in Supporting Information S1) (Kaufman et al., 2020), causing local temperature to dominate precipitation $\delta^2\text{H}$ variability. As the LIS margin retreated across Baffin Island throughout the Early Holocene, the anticyclonic circulation weakened and shifted inland of the mountain range that forms the spine of Baffin Island (Gregoire et al., 2018), allowing circulation around the GIS high-pressure system to dominate along the coast (Figures 1c and 1e). The TraCE-21k simulation supports this interpretation: even when the LIS was relatively large from 11 to 9 ka, the stronger high-pressure system over the GIS caused southeasterly winds to dominate in this region (Figures 1a–1c).

Glacier and paleoceanographic records from the Baffin Bay region indicate widespread climatic changes around 9.8 ka. An increase in background ice-rafter-debris delivery to the Labrador Sea (Figure 3e) may indicate continuous freshwater contributions from North American Ice Sheets, whereas previously, ice-rafter-debris occurred in distinct peaks (Jennings et al., 2015). Farther north, Baffin Bay shifted from permanent to seasonal sea-ice cover and to saltier surface water, suggesting less ice-sheet melt and more Atlantic-water influence (Figure 3d) (Gibb et al., 2015). Atlantic water reached the Canadian Arctic Archipelago by 10 ka (Pienkowski et al., 2013, 2014). In contrast to the oceanic records, which were experiencing the beginning of peak Holocene warmth, summers on the Agassiz Ice Cap, Ellesmere Island, had already begun to cool (Figure 3c) (Lecavalier et al., 2017). Like the Clyde Foreland, stable water isotopes in ice cores at Summit, Greenland suggest a shift to warmer (more remote) moisture sources between 10 and 8 ka, which remained relatively constant for the remainder of the Holocene (Masson-Delmotte et al., 2005). It is possible that this region-wide shift to full interglacial conditions, and the atmospheric circulation change captured in Greenland ice and Lake CF8, are due to the diminished strength of the LIS high-pressure system.

On centennial time scales, Lake CF8 summer temperature and precipitation $\delta^2\text{H}$ were not correlated after 9.8 ka. Southeasterly winds caused by the GIS high-pressure system were so dominant during this time that centennial-scale changes in their strength would not have influenced the direction of moisture delivery to Baffin Island (Figures 1b and 1c). These results suggest that the GIS high-pressure system dominated large-scale circulation from 9.8 to 7.5 ka, delivering remote moisture to the Baffin Bay region.

4.2.3. After 8 ka

Around 8.0 ka, summer precipitation on western Greenland and eastern Baffin Island became ${}^2\text{H}$ -enriched (Figure 2a) (Thomas et al., 2018). By about 8.5 ka, the LIS was small enough that its topography no longer impacted regional climate (Gregoire et al., 2018). Continued LIS retreat between 9 and 8 ka (Figure 3c) (Dalton et al., 2020) exposed ice-free land in the northeastern Canadian Arctic, meaning that summer circulation patterns similar to today began around this time (Figures 1f and 1g). The boreal forest migrated northward as the LIS retreated in central and eastern Canada (de Lafontaine & Payette, 2011; Strong & Hills, 2005). Thus, starting around 8.0 ka, evapotranspiration from abundant lakes and the boreal forest in central and eastern Canada may have caused a shift to local moisture sources and ${}^2\text{H}$ -enriched precipitation around Baffin Bay. A trend toward lower $\epsilon_{\text{terrestrial-aquatic}}$ values in both the Clyde Foreland and western Greenland (Figure 2b) may indicate a shift toward wetter summers coincident with the increase in local moisture supply (Thomas et al., 2018).

5. Summary and Conclusions

During the Younger Dryas and Early Holocene, the front between the LIS and GIS high-pressure systems was positioned over northeastern Baffin Island (Liu et al., 2009), making this region sensitive to atmospheric circulation changes associated with ice-sheet retreat (Figures 1a–1c, 3b and 3c). The relative strength and position of these high-pressure systems influenced the direction of summer atmospheric circulation on northeastern Baffin Island, which in turn impacted whether moisture sources were remote (${}^2\text{H}$ -depleted) or local (${}^2\text{H}$ -enriched). Because remote moisture to this region was derived from lower latitudes, ${}^2\text{H}$ -depleted precipitation coincided with relatively high temperatures, whereas ${}^2\text{H}$ -enriched local moisture was associated with lower temperatures. Thus, the anticorrelation between summer temperature and precipitation $\delta^2\text{H}$ for parts of the Early Holocene (Figures 3a and 3b) indicates rapid shifts between local and remote moisture sources. After 9.8 ka, summer temperature and precipitation $\delta^2\text{H}$ were strongly correlated, indicating a single dominant moisture source. We interpret this shift in moisture sources to be a threshold response by the atmosphere to the gradual retreat of the LIS.

Interpreting this summer precipitation $\delta^2\text{H}$ record in conjunction with an independent record of summer temperature yields information about atmospheric circulation that would not be discernible from individual temperature or precipitation $\delta^2\text{H}$ proxy records. This multi-proxy approach is especially useful to identify changing moisture sources, which caused an unexpected relationship between summer temperature and precipitation $\delta^2\text{H}$ values.

This study suggests that changes in continental ice sheet size and configuration influence atmospheric circulation on centennial to millennial time scales. Moreover, we find that gradual LIS retreat during the Early Holocene caused a threshold atmospheric response in the Baffin Bay region around 9.8 ka. Today, anticyclonic circulation around the GIS causes consistent strong northward moisture flux over the Labrador Sea (Dufour et al., 2016). Just as LIS retreat during the last deglaciation caused weaker anticyclonic circulation over North America, a smaller GIS may be associated with a weaker high-pressure system and reduced anticyclonic circulation. As the GIS retreats in coming centuries (P. U. Clark et al., 2016), rapid changes in the amount or location of moisture transport may occur. Additionally, ice sheet-atmosphere feedbacks may speed up GIS mass loss (Le clec'h et al., 2019).

In past interglacial periods, the GIS was likely smaller than present (de Vernal & Hillaire-Marcel, 2008; Schaefer et al., 2016), with potential impacts on moisture delivery to the Arctic. The handful of paleoclimate archives that span multiple interglacial periods in this region (Knutz et al., 2019; Miller et al., 2022; NEEM Community Members, 2013) offer an opportunity to use this multi-proxy approach to explore the nature and extent of these impacts.

Data Availability Statement

Samples archived at the University at Buffalo, new Lake CF8 data available at <https://doi.org/10.25921/r1dc-8930>, code available at <https://doi.org/10.5281/zenodo.7966589> and <https://doi.org/10.5281/zenodo.7702542>.

Acknowledgments

The University at Buffalo operates on the territory of the Seneca Nation, a member of the Haudenosaunee/Six Nations Confederacy. We thank the Qikitani Inuit who provided access to their land and logistical support for field work. We thank Aron Bini, JR Noble, James Qillaq, Joamie Qillaq, Monica Ridgeway, and Don Rodbell for field support, Martha Raynolds for vegetation data, Harald Sodemann, Hans Christian Steen-Larsen, and Iris Thurnherr for discussions about interpretations, and Ben Gaglioti and an anonymous reviewer for constructive reviews. This research was supported by NSF EAR PDRF 1349595, NSF EAR-IF 1652274, NSF ARCSS 1737716, NSF ARCSS 1947981, and a Fulbright Norway Scholar award to EKT; NSF AGS PDRF 2114657 to AAC; NSF ARCSS 1948005 to MPE and NPM.

References

- Allegretti, G., Carchini, G., Convey, P., & Sbordoni, V. (2012). Evolutionary geographic relationships among orthocladine chironomid midges from maritime Antarctic and sub-Antarctic islands. *Biological Journal of the Linnean Society*, 106(2), 258–274. <https://doi.org/10.1111/j.1095-8312.2012.01864.x>
- Arctic Report Card. (2022). Retrieved from https://www.arctic.noaa.gov/Portals/7/ArcticReportCard/Documents/ArcticReportCard_full_report2022.pdf
- Axford, Y., Briner, J. P., Miller, G. H., & Francis, D. R. (2009). Paleoecological evidence for abrupt cold reversals during peak Holocene warmth on Baffin Island, Arctic Canada. *Quaternary Research*, 71(2), 142–149. <https://doi.org/10.1016/j.yqres.2008.09.006>
- Axford, Y., de Vernal, A., & Osterberg, E. C. (2021). Past warmth and its impacts during the holocene thermal maximum in Greenland. *Annual Review of Earth and Planetary Sciences*, 49(1), 279–307. <https://doi.org/10.1146/annurev-earth-081420-063858>
- Berrisford, P., Dee, D. P., Poli, P., Brugge, R., Fielding, M., Fuentes, M., et al. (2011). *The ERA-Interim archive Version 2.0. ERA Report Series* (p. 23). ECMWF.
- Blaauw, M., & Christen, J. A. (2011). Flexible paleoclimate age-depth models using an autoregressive gamma process. *Bayesian Analysis*, 6(3), 457–474. <https://doi.org/10.1214/11-BA618>
- Blaga, C. I., Reichart, G.-J., Heiri, O., & Sinnighe Damsté, J. S. (2009). Tetraether membrane lipid distributions in water-column particulate matter and sediments: A study of 47 European lakes along a north–south transect. *Journal of Paleolimnology*, 41(3), 523–540. <https://doi.org/10.1007/s10933-008-9242-2>
- Bowen, G. J. (2016). OIPC: The online isotopes in precipitation calculator, version 2.2. Retrieved from www.waterisotopes.org
- Bowen, G. J., Wassenaar, L. I., & Hobson, K. A. (2005). Global application of stable hydrogen and oxygen isotopes to wildlife forensics. *Oecologia*, 143(3), 337–348. <https://doi.org/10.1007/s00442-004-1813-y>
- Briner, J. P., Axford, Y., Forman, S. L., Miller, G. H., & Wolfe, A. P. (2007). Multiple generations of interglacial lake sediment preserved beneath the Laurentide Ice Sheet. *Geology*, 35(10), 887. <https://doi.org/10.1130/G23812A.1>
- Briner, J. P., Davis, P. T., & Miller, G. H. (2009). Latest pleistocene and holocene glaciation of Baffin Island, Arctic Canada: Key patterns and chronologies. *Quaternary Science Reviews*, 28(21–22), 2075–2087. <https://doi.org/10.1016/j.quascirev.2008.09.017>
- Briner, J. P., Miller, G. H., Davis, P. T., & Finkel, R. C. (2005). Cosmogenic exposure dating in arctic glacial landscapes: Implications for the glacial history of northeastern Baffin Island, Arctic Canada. *Canadian Journal of Earth Sciences*, 42(1), 67–84. <https://doi.org/10.1139/e04-102>
- Bring, A., Fedorova, I., Dibike, Y., Hinzman, L., Mård, J., Mernild, S. H., et al. (2016). Arctic terrestrial hydrology: A synthesis of processes, regional effects, and research challenges. *Journal of Geophysical Research: Biogeosciences*, 121(3), 621–649. <https://doi.org/10.1002/2015JG003131>
- Buizert, C., Keisling, B. A., Box, J. E., He, F., Carlson, A. E., Sinclair, G., & DeConto, R. M. (2018). Greenland-wide seasonal temperatures during the last deglaciation. *Geophysical Research Letters*, 45(4), 1905–1914. <https://doi.org/10.1002/2017GL075601>
- Chen, Y., Zheng, F., Yang, H., Yang, W., Wu, R., Liu, X., et al. (2022). The production of diverse brGDGTs by an Acidobacterium providing a physiological basis for paleoclimate proxies. *Geochimica et Cosmochimica Acta*, 337, 155–165. <https://doi.org/10.1016/j.gca.2022.08.033>
- Chiasson-Poirier, G., Franssen, J., Lafrenière, M. J., Fortier, D., & Lamoureux, S. F. (2020). Seasonal evolution of active layer thaw depth and hillslope-stream connectivity in a permafrost watershed. *Water Resources Research*, 56(1). <https://doi.org/10.1029/2019WR025828>
- Clark, I. D., & Fritz, P. (1997). *Environmental isotopes in hydrogeology*. CRC Press. <https://doi.org/10.1201/9781482242911>
- Clark, P. U., Shakun, J. D., Marcott, S. A., Mix, A. C., Eby, M., Kulp, S., et al. (2016). Consequences of twenty-first-century policy for multi-millennial climate and sea-level change. *Nature Climate Change*, 6(4), 360–369. <https://doi.org/10.1038/nclimate2923>

- Cluett, A. A., Thomas, E. K., Castañeda, I. S., Cowling, O. C., & Morrill, C. (2023). Lake dynamics modulate the air temperature variability recorded by sedimentary aquatic biomarkers: A Holocene case study from western Greenland. *Journal of Geophysical Research: Biogeosciences*. <https://doi.org/10.1029/2022JG007106>
- Cluett, A. A., Thomas, E. K., Evans, S. M., & Keys, P. W. (2021). Seasonal Variations in moisture origin explain spatial contrast in precipitation isotope seasonality on coastal western Greenland. *Journal of Geophysical Research: Atmospheres*, 126(11), e2020JD033543. <https://doi.org/10.1029/2020JD033543>
- Crump, S. E., Fréchette, B., Power, M., Cutler, S., de Wet, G., Reynolds, M. K., et al. (2021). Ancient plant DNA reveals High Arctic greening during the Last Interglacial. *Proceedings of the National Academy of Sciences*, 118(13), e2019069118. <https://doi.org/10.1073/pnas.2019069118>
- Dalton, A. S., Margold, M., Stokes, C. R., Tarasov, L., Dyke, A. S., Adams, R. S., et al. (2020). An updated radiocarbon-based ice margin chronology for the last deglaciation of the North American Ice Sheet Complex. *Quaternary Science Reviews*, 234, 106223. <https://doi.org/10.1016/j.quascirev.2020.106223>
- Daniels, W. C., Castañeda, I. S., Salacup, J. M., Habicht, M. H., Lindberg, K. R., & Brigham-Grette, J. (2022). Archaeal lipids reveal climate-driven changes in microbial ecology at Lake El'gygytgyn (Far East Russia) during the Plio-Pleistocene. *Journal of Quaternary Science*, 37(5), 900–914. <https://doi.org/10.1002/jqs.3347>
- De Jonge, C., Hopmans, E. C., Zell, C. I., Kim, J.-H., Schouten, S., & Sinninghe Damsté, J. S. (2014). Occurrence and abundance of 6-methyl branched glycerol dialkyl glycerol tetraethers in soils: Implications for palaeoclimate reconstruction. *Geochimica et Cosmochimica Acta*, 141, 97–112. <https://doi.org/10.1016/j.gca.2014.06.013>
- De Jonge, C., Stadnitskaia, A., Hopmans, E. C., Cherkashov, G., Fedotov, A., & Sinninghe Damsté, J. S. (2014). In situ produced branched glycerol dialkyl glycerol tetraethers in suspended particulate matter from the Yenisei River, Eastern Siberia. *Geochimica et Cosmochimica Acta*, 125, 476–491. <https://doi.org/10.1016/j.gca.2013.10.031>
- de Lafontaine, G., & Payette, S. (2011). Shifting zonal patterns of the southern boreal forest in eastern Canada associated with changing fire regime during the Holocene. *Quaternary Science Reviews*, 30(7–8), 867–875. <https://doi.org/10.1016/j.quascirev.2011.01.002>
- Delettre, Y. R. (1988). Chironomid wing length, dispersal ability and habitat predictability. *Ecography*, 11(3), 166–170. <https://doi.org/10.1111/j.1600-0587.1988.tb00796.x>
- Denton, G. H., Alley, R. B., Comer, G. C., & Broecker, W. S. (2005). The role of seasonality in abrupt climate change. *Quaternary Science Reviews*, 24(10–11), 1159–1182. <https://doi.org/10.1016/j.quascirev.2004.12.002>
- de Vernal, A., & Hillaire-Marcel, C. (2008). Natural variability of Greenland climate, vegetation, and ice volume during the past million years. *Science*, 320(5883), 1622–1625. <https://doi.org/10.1126/science.1153929>
- de Wet, G. A., Castañeda, I. S., DeConto, R. M., & Brigham-Grette, J. (2016). A high-resolution mid-Pleistocene temperature record from Arctic Lake El'gygytgyn: A 50 kyr super interglacial from MIS 33 to MIS 31? *Earth and Planetary Science Letters*, 436, 56–63. <https://doi.org/10.1016/j.epsl.2015.12.021>
- Dufour, A., Zolina, O., & Gulev, S. K. (2016). Atmospheric moisture transport to the Arctic: Assessment of reanalyses and analysis of transport components. *Journal of Climate*, 29(14), 5061–5081. <https://doi.org/10.1175/JCLI-D-15-0559.1>
- Environment and Climate Change Canada. (2011). Canadian climate normals 1971–2000 station data—Climate—Environment and Climate Change Canada. Retrieved from https://climate.meteo.gc.ca/climate_normals/results_e.html?searchType=stnName&txtStationName=clyde&searchMethod=contains&txtCentralLatMin=0&txtCentralLatSec=0&txtCentralLongMin=0&txtCentralLongSec=0&stnID=1743&displayBack=1&month1=0&month2=12
- Faber, A.-K., Möllerø Vinther, B., Sjolte, J., & Anker Pedersen, R. (2017). How does sea ice influence $\delta^{18}\text{O}$ of Arctic precipitation? *Atmospheric Chemistry and Physics*, 17(9), 5865–5876. <https://doi.org/10.5194/acp-17-5865-2017>
- Francis, D. R., Wolfe, A. P., Walker, I. R., & Miller, G. H. (2006). Interglacial and Holocene temperature reconstructions based on midge remains in sediments of two lakes from Baffin Island, Nunavut, Arctic Canada. *Palaeogeography, Palaeoclimatology, Palaeoecology*, 236(1–2), 107–124. <https://doi.org/10.1016/j.palaeo.2006.01.005>
- Gaglioti, B. V., Mann, D. H., Wooller, M. J., Jones, B. M., Wiles, G. C., Groves, P., et al. (2017). Younger-Dryas cooling and sea-ice feedbacks were prominent features of the Pleistocene-Holocene transition in Arctic Alaska. *Quaternary Science Reviews*, 169, 330–343. <https://doi.org/10.1016/j.quascirev.2017.05.012>
- Gao, L., Hou, J., Toney, J., MacDonald, D., & Huang, Y. (2011). Mathematical modeling of the aquatic macrophyte inputs of mid-chain n-alkyl lipids to lake sediments: Implications for interpreting compound specific hydrogen isotopic records. *Geochimica et Cosmochimica Acta*, 75(13), 3781–3791. <https://doi.org/10.1016/j.gca.2011.04.008>
- Gibb, O. T., Steinbauer, S., Fréchette, B., de Vernal, A., & Hillaire-Marcel, C. (2015). Diachronous evolution of sea surface conditions in the Labrador Sea and Baffin Bay since the last deglaciation. *The Holocene*, 25(12), 1882–1897. <https://doi.org/10.1177/0959683615591352>
- Gibson, J. J., & Edwards, T. W. D. (2002). Regional water balance trends and evaporation-transpiration partitioning from a stable isotope survey of lakes in northern Canada. *Global Biogeochemical Cycles*, 16(2), 10–1–10–14. <https://doi.org/10.1029/2001GB001839>
- Gimeno, L., Eiras-Barca, J., Durán-Quesada, A. M., Domínguez, F., van der Ent, R., Sodemann, H., et al. (2021). The residence time of water vapour in the atmosphere. *Nature Reviews Earth & Environment*, 2(8), 558–569. <https://doi.org/10.1038/s43017-021-00181-9>
- Gorbey, D. B., Thomas, E. K., Sauer, P. E., Reynolds, M. K., Miller, G. H., Corcoran, M. C., et al. (2022). Modern eastern Canadian Arctic lake water isotopes exhibit latitudinal patterns in inflow seasonality and minimal evaporative enrichment. *Paleoceanography and Paleoclimatology*, 37(5), e2021PA004384. <https://doi.org/10.1029/2021PA004384>
- Green, A. J., & Sánchez, M. I. (2006). Passive internal dispersal of insect larvae by migratory birds. *Biology Letters*, 2(1), 55–57. <https://doi.org/10.1098/rsbl.2005.0413>
- Gregoire, L. J., Ivanovic, R. F., Maycock, A. C., Valdes, P. J., & Stevenson, S. (2018). Holocene lowering of the Laurentide ice sheet affects North Atlantic gyre circulation and climate. *Climate Dynamics*, 51(9), 3797–3813. <https://doi.org/10.1007/s00382-018-4111-9>
- Griggs, C. B., Lewis, C. F. M., & Kristovich, D. A. (2022). A late-glacial lake-effect climate regime and abundant tamarack in the Great Lakes Region, North America. *Quaternary Research*, 109, 1–19. <https://doi.org/10.1017/qua.2021.76>
- Guo, C.-Q., Ochyra, R., Wu, P.-C., Seppelt, R. D., Yao, Y.-F., Bian, L.-G., et al. (2013). Warnstorffia exannulata, an aquatic moss in the Arctic: Seasonal growth responses. *Climatic Change*, 119(2), 407–419. <https://doi.org/10.1007/s10584-013-0724-5>
- Halamka, T. A., Raberg, J. H., McFarlin, J. M., Younkin, A. D., Mulligan, C., Liu, X.-L., & Kopf, S. H. (2023). Production of diverse brGDGTs by Acidobacter Solibacter usitatus in response to temperature, pH, and O_2 provides a culturing perspective on brGDGT proxies and biosynthesis. *Geobiology*, 21(1), 102–118. <https://doi.org/10.1111/gbi.12525>
- He, C., Liu, Z., Otto-Biesner, B. L., Brady, E. C., Zhu, C., Tomas, R., et al. (2021). Abrupt Heinrich Stadial 1 cooling missing in Greenland oxygen isotopes. *Science Advances*, 7(25), eabih1007. <https://doi.org/10.1126/sciadv.abh1007>

- Hersbach, H., Bell, B., Berrisford, P., Hirahara, S., Horányi, A., Muñoz-Sabater, J., et al. (2020). The ERA5 global reanalysis. *Quarterly Journal of the Royal Meteorological Society*, 146(730), 1999–2049. <https://doi.org/10.1002/qj.3803>
- Hollister, K. V., Thomas, E. K., Raynolds, M. K., Bültmann, H., Raberg, J. H., Miller, G. H., et al. (2022). Aquatic and terrestrial plant contributions to sedimentary plant waxes in a modern Arctic lake setting. *Journal of Geophysical Research: Biogeosciences*, 127(8), e2022JG006903. <https://doi.org/10.1029/2022JG006903>
- Hopmans, E. C., Schouten, S., & Sinninghe Damsté, J. S. (2016). The effect of improved chromatography on GDGT-based palaeoproxies. *Organic Geochemistry*, 93, 1–6. <https://doi.org/10.1016/j.orggeochem.2015.12.006>
- Hopmans, E. C., Weijers, J. W. H., Schefuß, E., Herfort, L., Sinninghe Damsté, J. S., & Schouten, S. (2004). A novel proxy for terrestrial organic matter in sediments based on branched and isoprenoid tetraether lipids. *Earth and Planetary Science Letters*, 224(1), 107–116. <https://doi.org/10.1016/j.epsl.2004.05.012>
- Huguet, C., Hopmans, E. C., Febo-Ayala, W., Thompson, D. H., Sinninghe Damsté, J. S., & Schouten, S. (2006). An improved method to determine the absolute abundance of glycerol dibiphytanyl glycerol tetraether lipids. *Organic Geochemistry*, 37(9), 1036–1041. <https://doi.org/10.1016/j.orggeochem.2006.05.008>
- IAEA/WMO. (2011). *Global network of isotopes in precipitation*. The GNIP Database. Retrieved from <http://www.iaea.org/water>
- Jennings, A. E., Andrews, J., Pearce, C., Wilson, L., & Ólafsdóttir, S. (2015). Detrital carbonate peaks on the Labrador shelf, a 13–7ka template for freshwater forcing from the Hudson Strait outlet of the Laurentide Ice Sheet into the subpolar gyre. *Quaternary Science Reviews*, 107, 62–80. <https://doi.org/10.1016/j.quascirev.2014.10.022>
- Johnsen, S. J., Dahl-Jensen, D., Gundestrup, N., Steffensen, J. P., Clausen, H. B., Miller, H., et al. (2001). Oxygen isotope and paleotemperature records from six Greenland ice-core stations: Camp Century, Dye-3, GRIP, GISP2, Renland and NorthGRIP. *Journal of Quaternary Science*, 16(4), 299–307. <https://doi.org/10.1002/jqs.622>
- Jonsson, C. E., Leng, M. J., Rosqvist, G. C., Seibert, J., & Arrowsmith, C. (2009). Stable oxygen and hydrogen isotopes in sub-Arctic lake waters from northern Sweden. *Journal of Hydrology*, 376(1–2), 143–151. <https://doi.org/10.1016/j.jhydrol.2009.07.021>
- Kageyama, M., & Valdes, P. J. (2000). Impact of the North American ice-sheet orography on the Last Glacial Maximum eddies and snowfall. *Geophysical Research Letters*, 27(10), 1515–1518. <https://doi.org/10.1029/1999GL011274>
- Kaiser, H. F. (1958). The varimax criterion for analytic rotation in factor analysis. *Psychometrika*, 23(3), 187–200. <https://doi.org/10.1007/BF02289233>
- Kaufman, D. S., McKay, N. P., Routson, C. C., Erb, M. P., Davis, B., Heiri, O., et al. (2020). A global database of Holocene paleotemperature records. *Scientific Data*, 7(1), 1–34. <https://doi.org/10.1038/s41597-020-0445-3>
- Keisling, B. A., Castañeda, I. S., & Brigham-Grette, J. (2017). Hydrological and temperature change in Arctic Siberia during the intensification of Northern Hemisphere Glaciation. *Earth and Planetary Science Letters*, 457, 136–148. <https://doi.org/10.1016/j.epsl.2016.09.058>
- Knutz, P. C., Newton, A. M. W., Hopper, J. R., Huuse, M., Gregersen, U., Sheldon, E., & Dybkjær, K. (2019). Eleven phases of Greenland Ice Sheet shelf-edge advance over the past 2.7 million years. *Nature Geoscience*, 12(5), 361–368. <https://doi.org/10.1038/s41561-019-0340-8>
- Kobashi, T., Menkveld, L., Jeltsch-Thömmes, A., Vinther, B. M., Box, J. E., Muscheler, R., et al. (2017). Volcanic influence on centennial to millennial Holocene Greenland temperature change. *Scientific Reports*, 7(1), 1441. <https://doi.org/10.1038/s41598-017-01451-7>
- Kopeć, B. G., Lauder, A. M., Posmentier, E. S., & Feng, X. (2014). The diel cycle of water vapor in west Greenland. *Journal of Geophysical Research: Atmospheres*, 119(15), 9399. <https://doi.org/10.1002/2014JD021859>
- Kusch, S., Winterfeld, M., Mollenhauer, G., Höfle, S. T., Schirrmeister, L., Schwamborn, G., & Rethemeyer, J. (2019). Glycerol dialkyl glycerol tetraethers (GDGTs) in high latitude Siberian permafrost: Diversity, environmental controls, and implications for proxy applications. *Organic Geochemistry*, 136, 103888. <https://doi.org/10.1016/j.orggeochem.2019.06.009>
- Lecavalier, B. S., Fisher, D. A., Milne, G. A., Vinther, B. M., Tarasov, L., Huybrechts, P., et al. (2017). High Arctic Holocene temperature record from the Agassiz ice cap and Greenland ice sheet evolution. *Proceedings of the National Academy of Sciences*, 114(23), 5952–5957. <https://doi.org/10.1073/pnas.1616287114>
- Le clec'h, S., Charbit, S., Quiquet, A., Fettweis, X., Dumas, C., Kageyama, M., et al. (2019). Assessment of the Greenland ice sheet–atmosphere feedbacks for the next century with a regional atmospheric model coupled to an ice sheet model. *The Cryosphere*, 13(1), 373–395. <https://doi.org/10.5194/tc-13-373-2019>
- LeGrande, A. N., & Schmidt, G. A. (2009). Sources of Holocene variability of oxygen isotopes in paleoclimate archives. *Climate of the Past*, 5(3), 441–455. <https://doi.org/10.5194/cp-5-441-2009>
- Liakka, J., Löfverström, M., & Colleoni, F. (2016). The impact of the North American glacial topography on the evolution of the Eurasian ice sheet over the last glacial cycle. *Climate of the Past*, 12(5), 1225–1241. <https://doi.org/10.5194/cp-12-1225-2016>
- Lindberg, K. R., Daniels, W. C., Castañeda, I. S., & Brigham-Grette, J. (2022). Biomarker proxy records of Arctic climate change during the Mid-Pleistocene transition from Lake El'gygytgyn (Far East Russia). *Climate of the Past*, 18(3), 559–577. <https://doi.org/10.5194/cp-18-559-2022>
- Liu, Z., Otto-Btiesner, B. L., He, F., Brady, E. C., Tomas, R., Clark, P. U., et al. (2009). Transient simulation of last deglaciation with a new mechanism for Bolling-Allerod warming. *Science*, 325(5938), 310–314. <https://doi.org/10.1126/science.1171041>
- Livingstone, D. M., & Lotter, A. F. (1998). The relationship between air and water temperatures in lakes of the Swiss Plateau: A case study with paleolimnological implications. *Journal of Paleolimnology*, 19(2), 181–198. <https://doi.org/10.1023/A:1007904817619>
- Löfverström, M., Caballero, R., Nilsson, J., & Kleman, J. (2014). Evolution of the large-scale atmospheric circulation in response to changing ice sheets over the last glacial cycle. *Climate of the Past*, 10(4), 1453–1471. <https://doi.org/10.5194/cp-10-1453-2014>
- MacIntyre, S., Fram, J. P., Kushner, P. J., Bettez, N. D., O'Brien, W. J., Hobbs, J. E., & Kling, G. W. (2009). Climate-related variations in mixing dynamics in an Alaskan arctic lake. *Limnology and Oceanography*, 54(6part2), 2401–2417. https://doi.org/10.4319/lo.2009.54.6_part_2.2401
- Martínez-Sosa, P., & Tierney, J. E. (2019). Lacustrine brGDGT response to microcosm and mesocosm incubations. *Organic Geochemistry*, 127, 12–22. <https://doi.org/10.1016/j.orggeochem.2018.10.011>
- Martínez-Sosa, P., Tierney, J. E., Stefanescu, I. C., Dearing Crampton-Flood, E., Shuman, B. N., & Routson, C. (2021). A global Bayesian temperature calibration for lacustrine brGDGTs. *Geochimica et Cosmochimica Acta*, 305, 87–105. <https://doi.org/10.1016/j.gca.2021.04.038>
- Marzi, R., Torkelson, B. E., & Olson, R. K. (1993). A revised carbon preference index. *Organic Geochemistry*, 20(8), 1303–1306. [https://doi.org/10.1016/0146-6380\(93\)90016-5](https://doi.org/10.1016/0146-6380(93)90016-5)
- Masson-Delmotte, V., Jouzel, J., Landais, A., Stevenard, M., Johnsen, S. J., White, J. W. C., et al. (2005). GRIP deuterium excess reveals rapid and orbital-scale changes in Greenland moisture origin. *Science*, 309(5731), 118–121. <https://doi.org/10.1126/science.1108575>
- McAndrews, J. H. (1984). Pollen Analysis of the 1973 Ice Core from Devon Island Glacier, Canada. *Quaternary Research*, 22(1), 68–76. [https://doi.org/10.1016/0033-5894\(84\)90007-3](https://doi.org/10.1016/0033-5894(84)90007-3)
- McFarlin, J. M., Axford, Y., Masterson, A. L., & Osburn, M. R. (2019). Calibration of modern sedimentary δ_{2H} plant wax-water relationships in Greenland lakes. *Quaternary Science Reviews*, 225, 105978. <https://doi.org/10.1016/j.quascirev.2019.105978>

- McKay, N. P., Emile-Geay, J., & Khider, D. (2021). geoChronR—An R package to model, analyze, and visualize age-uncertain data. *Geochronology*, 3(1), 149–169. <https://doi.org/10.5194/gchron-3-149-2021>
- Miller, G. H., Wolfe, A. P., Axford, Y., Briner, J. P., Bueltmann, H., Crump, S., et al. (2022). Last interglacial lake sediments preserved beneath Laurentide and Greenland Ice sheets provide insights into Arctic climate amplification and constrain 130 ka of ice-sheet history. *Journal of Quaternary Science*, 37(5), 979–1005. <https://doi.org/10.1002/jqs.3433>
- Naafs, B. D. A., Inglis, G. N., Zheng, Y., Amesbury, M. J., Biester, H., Bindler, R., et al. (2017). Introducing global peat-specific temperature and pH calibrations based on brGDGT bacterial lipids. *Geochimica et Cosmochimica Acta*, 208, 285–301. <https://doi.org/10.1016/j.gca.2017.01.038>
- NEEM Community Members. (2013). Eemian interglacial reconstructed from a Greenland folded ice core. *Nature*, 493(7433), 489–494. <https://doi.org/10.1038/nature11789>
- Nusbaumer, J., Alexander, P. M., LeGrande, A. N., & Tedesco, M. (2020). Spatial shift of Greenland moisture sources related to enhanced Arctic warming. *Geophysical Research Letters*, 46(24), 14723–14731. <https://doi.org/10.1029/2019GL084633>
- Paterson, W. S. B., Koerner, R. M., Fisher, D., Johnsen, S. J., Clausen, H. B., Dansgaard, W., et al. (1977). An oxygen-isotope climatic record from the Devon Island ice cap, arctic Canada. *Nature*, 266(5602), 508–511. <https://doi.org/10.1038/266508a0>
- Pendleton, S., Miller, G., Lifton, N., & Young, N. (2019). Cryosphere response resolves conflicting evidence for the timing of peak Holocene warmth on Baffin Island, Arctic Canada. *Quaternary Science Reviews*, 216, 107–115. <https://doi.org/10.1016/j.quascirev.2019.05.015>
- Pieńkowski, A. J., England, J. H., Furze, M. F. A., Blasco, S., Mudie, P. J., & MacLean, B. (2013). 11,000 yrs of environmental change in the Northwest Passage: A multiproxy core record from central Parry Channel, Canadian High Arctic. *Marine Geology*, 341, 68–85. <https://doi.org/10.1016/j.margeo.2013.04.008>
- Pieńkowski, A. J., England, J. H., Furze, M. F. A., MacLean, B., & Blasco, S. (2014). The late Quaternary environmental evolution of marine Arctic Canada: Barrow Strait to Lancaster Sound. *Quaternary Science Reviews*, 91, 184–203. <https://doi.org/10.1016/j.quascirev.2013.09.025>
- Putman, A. L., Feng, X., Sonder, L. J., & Posmentier, E. S. (2017). Annual variation in event-scale precipitation $\delta^2\text{H}$ at Barrow, AK, reflects vapor source region. *Atmospheric Chemistry and Physics*, 17(7), 4627–4639. <https://doi.org/10.5194/acp-17-4627-2017>
- Raberg, J. H., Harning, D. J., Crump, S. E., de Wet, G., Blumm, A., Kopf, S., et al. (2021). Revised fractional abundances and warm-season temperatures substantially improve brGDGT calibrations in lake sediments. *Biogeosciences*, 18(12), 3579–3603. <https://doi.org/10.5194/bg-18-3579-2021>
- Rach, O., Brauer, A., Wilkes, H., & Sachse, D. (2014). Delayed hydrological response to Greenland cooling at the onset of the Younger Dryas in western Europe. *Nature Geoscience*, 7(2), 109–112. <https://doi.org/10.1038/ngeo2053>
- Reimer, P. J., Austin, W. E. N., Bard, E., Bayliss, A., Blackwell, P. G., Ramsey, C. B., et al. (2020). The IntCal20 Northern Hemisphere radiocarbon age calibration curve (0–55 cal kBP). *Radiocarbon*, 62(4), 725–757. <https://doi.org/10.1017/RDC.2020.41>
- Richman, M. B. (1986). Rotation of principal components. *Journal of Climatology*, 6(3), 293–335. <https://doi.org/10.1002/joc.3370060305>
- Rohling, E. J., & Pälike, H. (2005). Centennial-scale climate cooling with a sudden cold event around 8,200 years ago. *Nature*, 434(7036), 975–979. <https://doi.org/10.1038/nature03421>
- Russell, J. M., Hopmans, E. C., Loomis, S. E., Liang, J., & Sinnenhe Damsté, J. S. (2018). Distributions of 5- and 6-methyl branched glycerol dialkyl glycerol tetraethers (brGDGTs) in East African lake sediment: Effects of temperature, pH, and new lacustrine paleotemperature calibrations. *Organic Geochemistry*, 117, 56–69. <https://doi.org/10.1016/j.orggeochem.2017.12.003>
- Sachse, D., Billault, I., Bowen, G. J., Chikaraishi, Y., Dawson, T. E., Feakins, S. J., et al. (2012). Molecular paleohydrology: Interpreting the hydrogen-isotopic composition of lipid biomarkers from photosynthesizing organisms. *Annual Review of Earth and Planetary Sciences*, 40(1), 221–249. <https://doi.org/10.1146/annurev-earth-042711-105535>
- Schaefer, J. M., Finkel, R. C., Balco, G., Alley, R. B., Caffee, M. W., Briner, J. P., et al. (2016). Greenland was nearly ice-free for extended periods during the Pleistocene. *Nature*, 540(7632), 252–255. <https://doi.org/10.1038/nature20146>
- Schaetzl, R., Kris, F., Lewis, C., Luehmann, M., & Michalek, M. (2016). Spits formed in Glacial Lake Algonquin indicate strong easterly winds over the Laurentian Great Lakes during late Pleistocene. *Journal of Paleolimnology*, 55(1), 49–65. <https://doi.org/10.1007/s10933-015-9862-2>
- Schouten, S., Hopmans, E. C., & Sinnenhe Damsté, J. S. (2013). The organic geochemistry of glycerol dialkyl glycerol tetraether lipids: A review. *Organic Geochemistry*, 54, 19–61. <https://doi.org/10.1016/j.orggeochem.2012.09.006>
- Serreze, M. C., Barrett, A. P., Slater, A. G., Woodgate, R. A., Aagaard, K., Lammers, R. B., et al. (2006). The large-scale freshwater cycle of the Arctic. *Journal of Geophysical Research*, 111(C11), C11010. <https://doi.org/10.1029/2005JC003424>
- Shanahan, T. M., Huguen, K. A., & Van Mooy, B. A. S. (2013). Temperature sensitivity of branched and isoprenoid GDGTs in Arctic lakes. *Organic Geochemistry*, 64, 119–128. <https://doi.org/10.1016/j.orggeochem.2013.09.010>
- Singh, H. K. A., Bitz, C. M., Donohoe, A., & Rasch, P. J. (2017). A source–receptor perspective on the polar hydrologic cycle: Sources, seasonality, and Arctic–Antarctic parity in the hydrologic cycle response to CO_2 doubling. *Journal of Climate*, 30(24), 9999–10017. <https://doi.org/10.1175/JCLI-D-16-0917.1>
- Snyder, D. B., Berman, R. G., Kendall, J.-M., & Sanborn-Barrie, M. (2013). Seismic anisotropy and mantle structure of the Rae craton, central Canada: from joint interpretation of SKS splitting and receiver functions. *Precambrian Research*, 232, 189–208. <https://doi.org/10.1016/j.precamres.2012.03.003>
- Sodemann, H., Masson-Delmotte, V., Schwierz, C., Vinther, B. M., & Wernli, H. (2008). Interannual variability of Greenland winter precipitation sources: 2. Effects of North Atlantic Oscillation variability on stable isotopes in precipitation. *Journal of Geophysical Research*, 113(D12), D12111. <https://doi.org/10.1029/2007JD009416>
- Steen-Larsen, H. C., Sveinbjörnsdóttir, A. E., Jonsson, T., Ritter, F., Bonne, J.-L., Masson-Delmotte, V., et al. (2015). Moisture sources and synoptic to seasonal variability of North Atlantic water vapor isotopic composition. *Journal of Geophysical Research: Atmospheres*, 120(12), 5757–5774. <https://doi.org/10.1002/2015JD023234>
- Strong, W. L., & Hills, L. V. (2005). Late-glacial and Holocene palaeovegetation zonal reconstruction for central and north-central North America. *Journal of Biogeography*, 32(6), 1043–1062. <https://doi.org/10.1111/j.1365-2699.2004.01223.x>
- Thomas, E. K., Castañeda, I. S., McKay, N. P., Briner, J. P., Salacup, J. M., Nguyen, K. Q., & Schweinsberg, A. D. (2018). A wetter Arctic coincident with hemispheric warming 8,000 years ago. *Geophysical Research Letters*, 45(19), 10637–10647. <https://doi.org/10.1029/2018GL079517>
- Thomas, E. K., Clemens, S. C., Prell, W. L., Herbert, T. D., Huang, Y., Liu, Z., et al. (2014). Temperature and leaf wax $\delta^{13}\text{C}$ records demonstrate seasonal and regional controls on Asian monsoon proxies. *Geology*, 42(12), 1075–1078. <https://doi.org/10.1130/G36289.1>
- Thomas, E. K., Hollister, K. V., Cluett, A. A., & Corcoran, M. C. (2020). Reconstructing Arctic precipitation seasonality using aquatic leaf wax $\delta^{13}\text{C}$ in lakes with contrasting residence times. *Paleoceanography and Paleoclimatology*, 35(7), e2020PA003886. <https://doi.org/10.1029/2020PA003886>
- Tulenko, J. P., Lofverstrom, M., & Briner, J. P. (2020). Ice sheet influence on atmospheric circulation explains the patterns of Pleistocene alpine glacier records in North America. *Earth and Planetary Science Letters*, 534, 116115. <https://doi.org/10.1016/j.epsl.2020.116115>

- van Bree, L. G. J., Peterse, F., van der Meer, M. T. J., Middelburg, J. J., Negash, A. M. D., De Crop, W., et al. (2018). Seasonal variability in the abundance and stable carbon-isotopic composition of lipid biomarkers in suspended particulate matter from a stratified equatorial lake (Lake Chala, Kenya/Tanzania): Implications for the sedimentary record. *Quaternary Science Reviews*, 192, 208–224. <https://doi.org/10.1016/j.quascirev.2018.05.023>
- Vihma, T., Screen, J., Tjernström, M., Newton, B., Zhang, X., Popova, V., et al. (2016). The atmospheric role in the Arctic water cycle: A review on processes, past and future changes, and their impacts. *Journal of Geophysical Research: Biogeosciences*, 121(3), 586–620. <https://doi.org/10.1002/2015JG003132>
- Vinnikov, K. Y., Yu, Y., Goldberg, M. D., Chen, M., & Tarpley, D. (2011). Scales of temporal and spatial variability of midlatitude land surface temperature. *Journal of Geophysical Research*, 116(D2), D02105. <https://doi.org/10.1029/2010JD014868>
- White, J. W. C., Barlow, L. K., Fisher, D., Grootes, P., Jouzel, J., Johnsen, S. J., et al. (1997). The climate signal in the stable isotopes of snow from Summit, Greenland: Results of comparisons with modern climate observations. *Journal of Geophysical Research*, 102(C12), 26425–26439. <https://doi.org/10.1029/97JC00162>
- Wilson, C. R., Michelutti, N., Cooke, C. A., Briner, J. P., Wolfe, A. P., & Smol, J. P. (2012). Arctic lake ontogeny across multiple interglaciations. *Quaternary Science Reviews*, 31, 112–126. <https://doi.org/10.1016/j.quascirev.2011.10.018>
- Wolfe, A. P., Miller, G. H., Olsen, C. A., Forman, S. L., Doran, P. T., & Holmgren, S. U. (2004). Geochronology of high latitude lake sediments. In R. Pienitz, M. S. V. Douglas, & J. P. Smol (Eds.), *Long-term environmental change in Arctic and Antarctic lakes* (pp. 19–52). Springer. Retrieved from <http://www.springer.com/environment/global+change++climate+change/book/978-1-4020-2125-1>
- Wu, J., Yang, H., Pancost, R. D., Naafs, B. D. A., Qian, S., Dang, X., et al. (2021). Variations in dissolved O₂ in a Chinese lake drive changes in microbial communities and impact sedimentary GDGT distributions. *Chemical Geology*, 579, 120348. <https://doi.org/10.1016/j.chemgeo.2021.120348>
- Yao, Y., Zhao, J., Vachula, R. S., Werne, J. P., Wu, J., Song, X., & Huang, Y. (2020). Correlation between the ratio of 5-methyl hexamethylated to pentamethylated branched GDGTs (HP5) and water depth reflects redox variations in stratified lakes. *Organic Geochemistry*, 147, 104076. <https://doi.org/10.1016/j.orggeochem.2020.104076>
- Young, N. E., Briner, J. P., Miller, G. H., Lesnek, A. J., Crump, S. E., Thomas, E. K., et al. (2020). Deglaciation of the Greenland and Laurentide ice sheets interrupted by glacier advance during abrupt coolings. *Quaternary Science Reviews*, 229, 106091. <https://doi.org/10.1016/j.quascirev.2019.106091>
- Young, N. E., Briner, J. P., Rood, D. H., & Finkel, R. C. (2012). Glacier extent during the Younger Dryas and 8.2-ka event on Baffin Island, Arctic Canada. *Science*, 337(6100), 1330–1333. <https://doi.org/10.1126/science.1222759>
- Zhang, Z., Smitenberg, R. H., & Bradley, R. S. (2016). GDGT distribution in a stratified lake and implications for the application of TEX₈₆ in paleoenvironmental reconstructions. *Scientific Reports*, 6(1), 34465. <https://doi.org/10.1038/srep34465>
- Zhao, B., Castañeda, I. S., Bradley, R. S., Salacup, J. M., de Wet, G. A., Daniels, W. C., & Schneider, T. (2021). Development of an in situ branched GDGT calibration in Lake 578, southern Greenland. *Organic Geochemistry*, 152, 104168. <https://doi.org/10.1016/j.orggeochem.2020.104168>
- Zhao, B., Castañeda, I. S., Salacup, J. M., Thomas, E. K., Daniels, W. C., Schneider, T., et al. (2022). Prolonged drying trend coincident with the demise of Norse settlement in southern Greenland. *Science Advances*, 8(12), eabm4346. <https://doi.org/10.1126/sciadv.abm4346>